

## Surface electronic and atomic structure of ErSi<sub>1.7</sub> on Si(111)

L. Stauffer, A. Mharchi, S. Saintenoy, C. Pirri, P. Wetzel, D. Bolmont, and G. Gewinner  
*Laboratoire de Physique et de Spectroscopie Electronique, Faculté des Sciences et Techniques, 4 rue des Frères Lumière,  
 68093 Mulhouse Cedex, France*

(Received 13 December 1994; revised manuscript received 25 July 1995)

The surface atomic and electronic structure of ErSi<sub>1.7</sub> layers epitaxially grown on Si(111) is studied by angle-resolved ultraviolet photoemission spectroscopy. The experimental results are compared to electronic band-structure calculations for various reasonable surface atomic configurations. Satisfactory agreement is obtained for two geometries consisting of reconstructed ErSi<sub>1.7</sub> (0001) surfaces. Both reconstructions involve a buckled Si top layer similar to (111) double layers in bulk Si but differ in their registries with respect to the bulk silicide layer underneath, leading to a silicide surface termination with ErSi<sub>1.7</sub> stoichiometry. In contrast, the calculations clearly show that a surface termination with ErSi<sub>1.7</sub> stoichiometry involving an ordered array of vacancies in the buckled Si top layer would result in a quite different surface electronic structure incompatible with the experimental one. This allows us to rule out this model often invoked in previous work. Finally, models exposing a bulklike flat Si graphitelike top layer, with or without vacancies, can also safely be ruled out on the basis of the present data.

### I. INTRODUCTION

Much interest has recently been devoted to the study of rare-earth (RE)/silicon interfaces. The reason for this interest is the discovery of very exciting properties of these systems, such as epitaxial growth on Si(111) and unique low Schottky barrier height on *n*-type silicon.<sup>1,2</sup> A detailed knowledge of the electronic and atomic structure of the silicide surface is required for the understanding of many processes in molecular-beam epitaxy. It is known that surface structure imposes significant constraints on the growth of thicker films. Hellman and Tung<sup>3</sup> have shown the possibility of altering the orientation of epitaxial Si layers grown on CoSi<sub>2</sub>(111) by manipulating the surface structure of the CoSi<sub>2</sub> layer.

Actually, RE silicides and, in particular, erbium disilicide have been extensively studied,<sup>1,2,4-6</sup> but the atomic structure of the silicide surface is not well established. The Er disilicide crystallizes in a hexagonal phase based on the AlB<sub>2</sub> structure. Along the [0001] direction, the structure consists of a stack of alternating (0001) hexagonal Er planes and graphitelike Si planes. The disilicide composition has been measured to be Si deficient yielding a nonstoichiometric ErSi<sub>2-x</sub> (*x* ~ 0.3) form. This results from ordered vacancies in the Si sublattice: one Si atom out of six is missing in the Si planes, which gives  $\sqrt{3} \times \sqrt{3}$  R 30° in-plane mesh, as observed by low-energy electron diffraction (LEED). The driving force, which causes the formation of vacancies, is apparently the compressive strain present in ideal graphitelike Si(0001) planes. These planes are made of hexagonal Si rings, with an interatomic distance of 2.18 Å, as compared to 2.35 Å in bulk Si. Therefore, expulsion of one out of six Si species and relaxation is one way to reduce this strain.

In recent papers,<sup>7-9</sup> we have demonstrated that one ML of Er deposited onto Si(111) at room temperature (RT) followed by annealing at 400 °C is converted into an

epitaxial *p*(1×1) two-dimensional (2D) disilicide layer with a high degree of crystalline order. It was possible to completely determine the structure of this single layer silicide. We arrived at the conclusion that Er forms an ordered hexagonal monolayer accommodated underneath a Si top layer similar to substrate Si(111) bilayers. The top layer geometry can be derived simply from a single ErSi<sub>2</sub> layer, with AlB<sub>2</sub> structure, by a buckling of the graphitelike Si(0001) plane. Only domains of *B*-type orientation are actually formed, i.e., the buckled layer is rotated by 180° around the surface normal with respect to the bilayers of the Si(111) substrate. Note that the *p*(1×1) LEED pattern indicates that this top layer Si surface does not involve vacancies in contrast with its nonbuckled Si(0001) counterpart in bulk ErSi<sub>1.7</sub>.

A main topic still under debate is the controversy about the epitaxial bulklike  $\sqrt{3} \times \sqrt{3}$  R 30° ErSi<sub>1.7</sub> silicide surface atomic structure. Actually, essentially two ErSi<sub>1.7</sub> surface structures have been put forward in the literature. Both models exhibit an ErSi<sub>1.7</sub>(0001) surface reconstruction made of a buckled layer of Si atoms, with a geometry similar to a Si(111) bilayer, instead of the graphitelike Si termination expected for a simple truncation of the bulk structure. In the first model, commonly adopted in the literature, a  $\sqrt{3} \times \sqrt{3}$  R 30° ordered array of Si vacancies is located on the outermost Si plane leading to a surface termination with the same ErSi<sub>1.7</sub> stoichiometry as in bulk.<sup>10,11</sup> The second model adopts the same surface reconstruction as found for 2D silicide, namely, a buckled Si top layer without vacancies leading to a surface termination of ErSi<sub>1.7</sub>(0001) with ErSi<sub>2</sub> stoichiometry.<sup>12,13</sup>

The former model was first proposed by Baptist *et al.*<sup>10</sup> who studied the growth of epitaxial YSi<sub>1.7</sub> layers on Si(111), using x-ray photoelectron diffraction. Epitaxial yttrium disilicide also crystallizes in the defective AlB<sub>2</sub> structure and yttrium is often considered as a RE in its physicochemical properties. Therefore, in analogy to epi-

taxially grown yttrium silicide, the  $\sqrt{3} \times \sqrt{3} R 30^\circ$  ErSi<sub>1.7</sub> LEED pattern has been attributed in previous work<sup>11</sup> to a vacancy array in the Si surface plane.

Investigation of the surface electronic structure of  $\sqrt{3} \times \sqrt{3} R 30^\circ$  ErSi<sub>1.7</sub> layers by means of high-resolution angle-resolved ultraviolet photoelectron spectroscopy (ARUPS) experiments<sup>12</sup> clearly supports the surface atomic structure relevant to the second model. It was found that typical surface bands of  $\sqrt{3} \times \sqrt{3} R 30^\circ$  ErSi<sub>1.7</sub> can be derived from the  $p(1 \times 1)$  2D silicide bands folded back into the reduced  $\sqrt{3} \times \sqrt{3}$  zone. In particular, we have provided physical arguments based on 2D Fermi-surface measurements, LEED observations, and electron counting that rule out the presence of vacancies in the buckled Si top layer. In contrast, no experimental or theoretical evidence that supports the presence of vacancies in the reconstructed Si top layer of bulklike ErSi<sub>1.7</sub> has been reported up to now.

The purpose of the present work is to discriminate between the above models by means of theoretical band-structure calculations. This approach has been very successful in previous work on the single Er silicide layer grown on Si(111).<sup>9</sup> In this work, we compared the experimental band structure to calculations by means of the extended Hückel theory (EHT) for a series of possible atomic arrangements. In spite of the approximate character of the EHT method, this work led to the correct atomic structure as determined later by Auger electron diffraction and surface extended x-ray-absorption fine structure (SEXAFS).<sup>8</sup> In a first approximation, the EHT method appears to be a very useful method that gives qualitatively correct trends, band topologies, and Fermi-level locations. This permits us to readily rule out many plausible structure models, in the case of complex compounds, without the heavy computations involved in more accurate theories. Here, we adopt the same approach to test a series of reasonable geometric surface structures of a 2 Er ML thick epitaxial ErSi<sub>1.7</sub> film (two silicide layers) on Si(111). As shown in previous works,<sup>12,14</sup> the surface electronic structure and the Schottky barrier height of bulklike ErSi<sub>1.7</sub> are already fully developed for layer thicknesses as small as two silicide layers. So, the study of a simple 2-ML silicide slab, most likely also gives information about the surface atomic and electronic structure of thicker silicide layers. The comparison of experimental and calculated bands clearly confirms the surface structure model of Ref. 12, i.e., a reconstructed Si top layer, *without vacancies* as ErSi<sub>1.7</sub> (0001) termination.

The paper is organized as follows. Section II recalls the experimental surface band structure determined in Ref. 12. In Sec. III A, we give an outline of the computational details and a description of the various tested structure models. In Sec. III B, we present the calculation results and compare them to the experimental ones. Finally, we summarize our conclusions in Sec. IV.

## II. EXPERIMENTAL BAND STRUCTURE

Figure 1(a) shows the dispersion of surface-state bands, located in the 0–1.7-eV binding-energy (BE) range, mea-

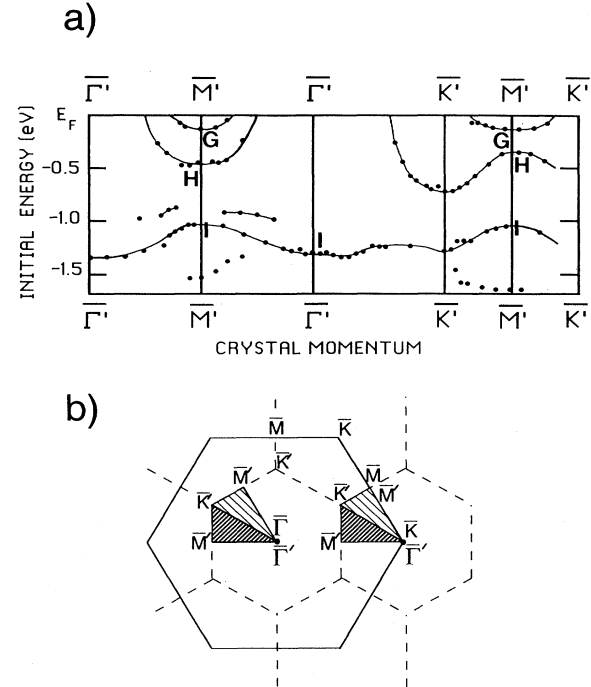


FIG. 1. (a) Dispersion of the experimental surface bands measured with He<sub>1</sub> photon energy on the 2 Er ML thick ErSi<sub>1.7</sub> silicide along the  $\bar{\Gamma}'\bar{M}'$  and  $\bar{\Gamma}'\bar{K}'$  symmetry lines of the  $\sqrt{3} \times \sqrt{3} R 30^\circ$  SBZ. The solid lines are guides to the eye to illustrate the band dispersions. (b) SBZ of epitaxial Er silicides. The solid and dashed lines denote the  $(1 \times 1)$  and  $\sqrt{3} \times \sqrt{3} R 30^\circ$  SBZ, respectively. The high-symmetry points labeled  $\bar{\Gamma}$ ,  $\bar{M}$ , and  $\bar{K}$  refer to the  $(1 \times 1)$  SBZ, whereas the  $\bar{\Gamma}'$ ,  $\bar{M}'$ , and  $\bar{K}'$  points refer to the  $\sqrt{3} \times \sqrt{3} R 30^\circ$  SBZ.

sured on a 2 ML Er thick ErSi<sub>1.7</sub> silicide layer, according to the ARUPS data, as established and discussed in detail in Refs. 12,14. Essentially, the same surface band structure is obtained for thicker (>2-ML) layers and the relevant surface structure is expected to be independent of Er coverage.<sup>12</sup> The calculations, however, are simpler and faster for a 2-ML silicide slab, so we are restricted to 2-ML films and it is reasonable to assume that the structural conclusions arrived at also hold for thicker layers. On the other hand, nearly perfect 2-ML films can be prepared with the method used in Ref. 12, according to recent scanning tunneling microscopy work.

The data are shown along the  $\bar{\Gamma}'\bar{M}'$  and  $\bar{\Gamma}'\bar{K}'\bar{M}'$  symmetry lines of the  $\sqrt{3} \times \sqrt{3} R 30^\circ$  surface Brillouin zone (SBZ). In Fig. 1(b), the high-symmetry points labeled  $\bar{\Gamma}$ ,  $\bar{M}$ , and  $\bar{K}$  refer to the  $(1 \times 1)$  SBZ, while the  $\bar{\Gamma}'$ ,  $\bar{M}'$ , and  $\bar{K}'$  refer to the  $(\sqrt{3} \times \sqrt{3} R 30^\circ)$  SBZ. The data display nicely the  $\sqrt{3} \times \sqrt{3}$  periodicity. In the following, we concentrate our discussion on three specific surface bands labeled *G*, *H*, and *I*, respectively, whose physical origin has been clearly established previously.<sup>12</sup> A nearly empty band (*G*) crosses the Fermi level near the  $\bar{M}'$  points, while a nearly filled one (*H*) crosses the Fermi level near the  $\bar{\Gamma}'$  points. A further surface band (*I*) has a maximum

BE of  $\sim 1.40$  eV at  $\bar{\Gamma}'$  and a minimum BE of  $\sim 1.00$  eV at  $\bar{M}'$ . We have demonstrated that these three surface bands, as well as the Fermi surface, can be qualitatively well understood in terms of back-folded 2D ErSi<sub>2</sub> silicide bands reflecting dangling-bond states of the buckled Si top layer. This means that bulklike ErSi<sub>1.7</sub> silicide and 2D ErSi<sub>2</sub> silicide must have similar surface terminations.

### III. CALCULATED BAND STRUCTURES

#### A. Computational method and models

The band structures are computed within the crystal-line extension of the EHT method. This method originating from quantum chemistry is similar to the tight-binding technique of physicists. In the present form of the EHT scheme, the periodic system is defined by a set of valence orbitals contained in a 2D unit cell and by two surface translation vectors. These atomic orbitals are described by Slater wave functions. The variational theorem leads to a generation of the secular determinant  $|H_{\mu\nu}(k) - E(k)S_{\mu\nu}(k)|$ , where the interaction elements  $H_{\mu\nu}(k)$  and the overlap integrals  $S_{\mu\nu}(k)$  are defined in terms of Bloch sums.  $E(k)$  is the energy associated with the orbital for a given  $k$  point. More details on the EHT method can be found in Refs. 15–17. The Fermi level  $E_F$  is obtained from a set of representative  $k$  points (uniform grid) in the irreducible part of the Brillouin zone affected by an appropriate weighting factor. We assume the Er configuration to be  $5d^{16}s^{24}f^{11}$ , with three valence electrons and ignore the corelike  $f$  electrons. Slater exponents and atomic energy levels are reported in Table I. Because of the large number of orbitals involved here, we neglect the Si  $d$  orbitals. This limitation slightly shifts down the energies, but does not modify the overall shape of the bands.

The slabs used in the calculations include two silicide layers and five Si(111) double layers from substrate. Test calculations show that adding further Si layers does not result in an appreciable change of the silicide-related bands. The dangling bonds left at the back face of the slab are saturated by one-orbital atoms (denoted BFA) so that a limited number of substrate layers provides a good simulation of the semi-infinite Si(111) crystal.

Basically, all tested structure models for the 2 Er ML thick silicide layer, include a graphitelike Si plane with a  $\sqrt{3} \times \sqrt{3}$   $R30^\circ$  ordered vacancy net sandwiched between two hexagonal Er planes. In all models, we assume that

the silicide-silicon interfacial geometry is the same as that determined for the 2D Er silicide,<sup>8,9</sup> namely, a  $T_4$  geometry, where Er atoms sit above the eclipsed hollow of the topmost Si(111) plane of the substrate. The vacancies in the graphitelike Si plane are located in the top site of the first Si(111) substrate plane. According to a previous SEXAFS investigation on epitaxial ErSi<sub>1.7</sub> silicide layers,<sup>18</sup> relaxation of the Si sublattice, due to the presence of vacancies, has been taken into account. A value of 0.20 Å has been assumed for the atomic displacement towards the vacancy site of the three-nearest-neighbor Si atoms surrounding a vacancy. The very small displacements of the Er from ideal AlB<sub>2</sub> position found in a recent structural study are neglected.<sup>19</sup>

The surface is made of an additional Si top layer, as shown in Fig. 2. Several surface atomic configurations, including nonreconstructed and reconstructed surfaces, have been considered in the calculations and are depicted in Fig. 3. All models consist of a bulklike ErSi<sub>1.7</sub> structure terminated by either a flat or a buckled Si top layer with or without vacancies. The atomic arrangement of models  $M_{1-4}$  include a buckled Si layer at the surface, with the same geometry as an ideal Si(111) (1×1) surface. Models  $M_1$  and  $M_2$  do not involve surface vacan-

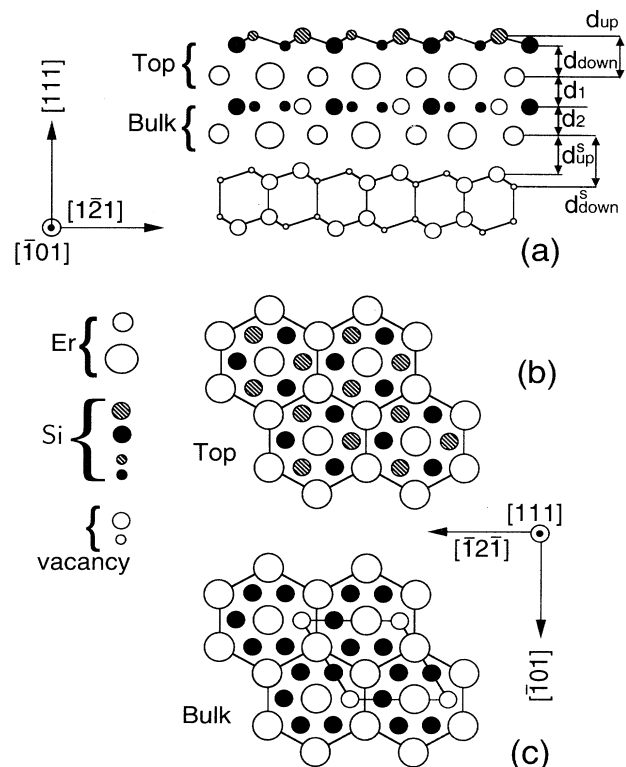


FIG. 2. Typical structure of the slab used in the band calculations for a 2 ML of Er disilicide. (a) Side view, the smaller circles indicate atoms lying out of the plane of the paper. (b) Sketch of reconstructed top silicide layer. (c) The underlying bulklike silicide layer. The Si substrate is modeled by an  $n$ -atomic-double-layer slab with backface dangling bonds saturated by one-orbital atoms.

TABLE I. Extended Hückel parameters [matrix elements  $H_{ii}$  (eV) and Slater exponents for Si and Er].

Orbital	$H_{ii}$ (eV)	Slater exponent
Er 6s	-4.882	1.396
Er 6p	-4.882	1.396
Er 5d	-6.917	2.199
Si 3s	-17.30	1.450
Si 3p	-9.20	1.450
BFA 3s	-11.20	1.450

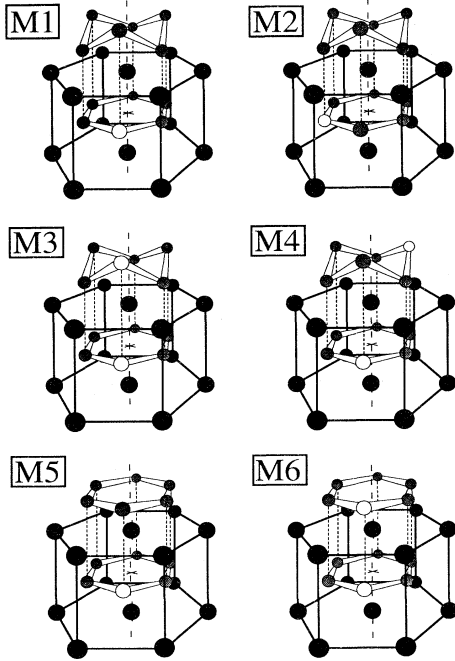


FIG. 3. Sketch of a series of plausible surface atomic configurations tested in the calculations. All models consist of a bulklike  $\text{ErSi}_{1.7}$  structure terminated with buckled ( $M_{1-4}$ ) or flat Si top layer ( $M_{5,6}$ ) and with ( $M_3, M_4, M_6$ ) or without vacancies ( $M_1, M_2, M_5$ ).

cies leading to a silicide surface termination that corresponds to the model proposed in Ref. 12. There are two inequivalent registries, where bulk Si vacancies are located below Si atoms of either the outermost (model  $M_1$ ) or inner plane (model  $M_2$ ) of the buckled Si top layer. In models  $M_3$  and  $M_4$ , the buckled Si top layer includes an ordered  $\sqrt{3} \times \sqrt{3} R30^\circ$  array of vacancies in the outermost layer according to the model of Refs. 10 and 11. In model  $M_3$  ( $M_4$ ), the surface vacancies are located above the vacancies (Si atoms) of the graphitelike Si plane underneath. Calculations were not performed for vacancies located in the inner plane of the buckled Si top layer, because this is energetically extremely unfavorable, since one additional dangling bond would then be introduced with respect to model  $M_3$  or  $M_4$ . In models  $M_5$  and  $M_6$ , we replace the buckled Si top layer by an unreconstructed graphitelike Si layer similar to the one in bulk silicide. Model  $M_5$  involves a Si top layer without vacancies, while model  $M_6$  corresponds to a nonreconstructed (0001) silicide surface with the same ordered net of vacancies as in bulk.

In principle, for all models shown in Fig. 3, more sophistication might be introduced by assuming a different relaxation, i.e., outward or inward shift, of the structurally inequivalent outermost Si atoms, according to their location above vacancies or Si atoms of the bulk Si graphitelike plane underneath. These two kinds of sites exhibit different electronic properties. However, one expects

only a slightly distorted version of the buckled Si top layer induced by the  $\sqrt{3}$  periodic potential, due to the underlying bulklike silicide layer. This is the reason why this higher-order effect has been neglected in a first approximation.

Figure 2 displays the typical structure of the slab corresponding to model  $M_1$  along with the structural parameters used in the band calculations. The  $d_{\text{up}}$  and  $d_{\text{down}}$  ( $d_{\text{down}}^S$  and  $d_{\text{up}}^S$ ) parameters show the interplanar distances between the buckled Si top layer (substrate layer) and the next Er plane, while  $d_1$  and  $d_2$  are the interplanar distances between the 2 Er planes and the graphitelike Si plane. According to previous works on 2D silicide,<sup>8,9</sup> we adopt the following parameters:  $d_{\text{down}} = 1.91 \text{ \AA}$ ;  $d_{\text{up}} = 2.71 \text{ \AA}$ ;  $d_{\text{down}}^S = 2.83 \text{ \AA}$ ;  $d_{\text{up}}^S = 2.05 \text{ \AA}$ ; and  $d_1 = d_2 = 2.045 \text{ \AA}$ .

### B. Results and comparison with experiments

The energy bands calculated along the  $\bar{\Gamma}'\bar{M}'$  direction of the  $\sqrt{3} \times \sqrt{3} R30^\circ$  SBZ for the various models are compared in Fig. 4. We concentrate here on the surface bands (heavy lines) denoted  $S_1, S_2, S_3$ , and  $S_4$  relevant to the states mainly localized in the Si top layer according to their orbital content. They are located in the 0–1.5-eV BE range. The other bands correspond either to bulklike silicide or Si substrate contributions.

Let us first consider the bands obtained from models  $M_1$  to  $M_4$  terminated by a buckled Si top layer. The shapes of bands  $S_1, S_2$ , and  $S_4$  are in qualitative agreement with the experimental bands  $G, H$ , and  $I$  and show the symmetry of the  $\sqrt{3} \times \sqrt{3} R30^\circ$  SBZ. However, their positions with respect to the Fermi level  $E_F$  change in a drastic way, depending on the specific atomic arrange-

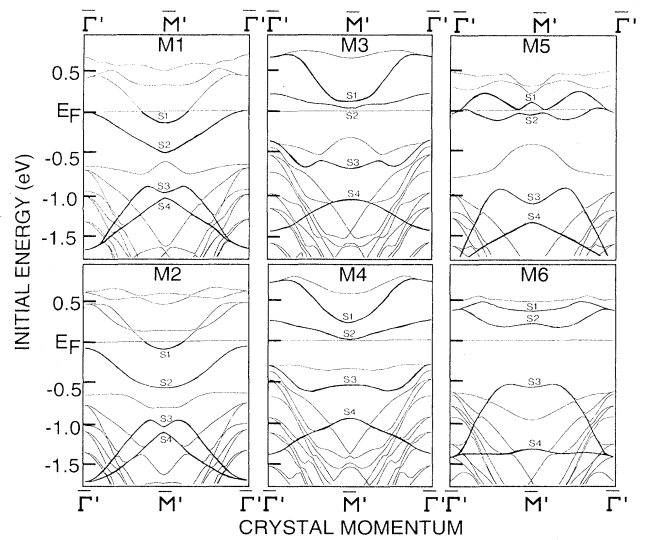


FIG. 4. Calculated bands for models  $M_1$ – $M_6$  along the  $\bar{\Gamma}'\bar{M}'$  line of the  $\sqrt{3} \times \sqrt{3} R30^\circ$  SBZ. The heavy lines labeled  $S_1, S_2, S_3$ , and  $S_4$  are surface bands relevant to states mainly localized in the Si top layer (Refs. 9 and 20).

ment. While models  $M_1$  and  $M_2$  obviously show reasonable agreement with experiment, the presence of a Si vacancy in the buckled Si top layer (models  $M_3$  or  $M_4$ ) results in the two upper bands  $S_1$  and  $S_2$  moving above the Fermi level and becoming unoccupied bands, in contrast with the corresponding bands obtained from model  $M_1$  or  $M_2$  and experiment. This difference can be qualitatively understood in a rigid-band model: if one removes one Si atom out of six in the top Si layer, there is a loss of valence electrons and bands  $S_1$  and  $S_2$ , which lie near  $E_F$  in model  $M_1$ , move towards higher energies with respect to  $E_F$ . Hence, the 2D Fermi surface is quite different from experiment. Note, however, that band  $S_4$ , more distant from  $E_F$ , is only slightly affected by the vacancies, indicating the limits of a rigid-band model. At any rate, the calculations show that the presence of vacancies in the buckled Si top layer is clearly incompatible with experiment and we rule out this hypothesis.

Let us now consider the energy bands obtained when we replace the buckled Si top layer by a flat unreconstructed Si layer (models  $M_5$  and  $M_6$ ). In model  $M_5$ , similar to bulk  $\text{ErSi}_2$ , we set  $d_{\text{up}} = d_{\text{down}} = 1.91 \text{ \AA}$ , with the other parameters unchanged. Comparing the relevant bands to those for models  $M_1$  or  $M_2$ , we immediately note drastic differences in the shape of the upper bands  $S_1$  and  $S_2$ . Both bands, which are now rather flat, present a minimum at  $\bar{\Gamma}'$  and extrema between  $\bar{\Gamma}'$  and  $\bar{M}'$ . The upper band is antibonding instead bonding at  $\bar{M}'$ . This topology is clearly incompatible with the experimental data and 2D Fermi surface.

Considering now the bands relevant to the model  $M_6$ , namely, a flat Si top layer with vacancies as in bulk  $\text{ErSi}_{1.7}$ , we observe again that the lower number of valence electrons results in empty bands  $S_1$  and  $S_2$ . Moreover, these bands are again quite flat and their topology differs drastically from experiment. We, therefore, also reject model  $M_6$ , which corresponds to an unreconstructed  $\text{ErSi}_{1.7}(0001)$  surface.

At this stage, it appears that structures involving a flat Si top layer with or without vacancies (models  $M_5$  and  $M_6$ ), as well as the hypothesis of a buckled Si top layer with vacancies (models  $M_3$  and  $M_4$ ), are incompatible with experiment. Only the surface energy bands calculated for the  $M_1$  and  $M_2$  geometries display the correct topology and 2D Fermi surface observed experimentally. Yet, it is clear that one cannot safely discriminate between models  $M_1$  and  $M_2$  on the basis of the present calculations, which yield very similar results. In Fig. 5, we compare in more detail experimental and calculated bands for model  $M_1$ . Both  $\bar{\Gamma}'\bar{K}'$  and  $\bar{\Gamma}'\bar{M}'$  directions are considered in this final step.

The agreement is qualitatively good, especially along  $\bar{\Gamma}'\bar{M}'$ . Bands  $S_1$ ,  $S_2$ , and  $S_4$  reproduce correctly the corresponding experimental bands  $G$ ,  $H$ , and  $I$ . We note, however, that band  $S_4$  presents more dispersion than band  $G$ . Similar discrepancies are observed in many instances, even with *ab initio* band calculations, and are partly related to the fact that photoemission measured excited states of the system, while the calculated bands are a ground-state property. Let us note, in this respect,

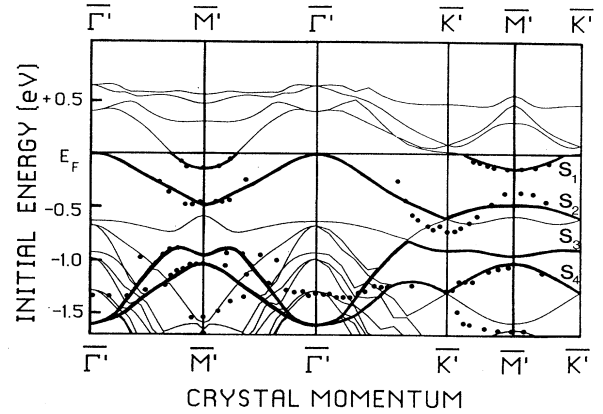


FIG. 5. Comparison of the experimental (solid dots) and calculated bands obtained for model  $M_1$  (full lines) along the  $\bar{\Gamma}'\bar{K}'$  and  $\bar{\Gamma}'\bar{M}'$  lines.

that all structural conclusions obtained in this work are based on a comparison of overall band topologies and fillings that are not expected to be strongly affected by more accurate calculations or self-energy corrections.

Finally, let us now consider the orbital nature of the relevant surface bands. We find that the orbital content of bands  $S_1$ ,  $S_2$ , and  $S_4$  is clearly reminiscent of that of the almost-empty and almost-filled bands calculated in the case of the epitaxial 2D Er silicide on  $\text{Si}(111)$ .<sup>9</sup>  $S_1$  shows hybridization between Er  $5d$  states from the two Er layers and Si  $3p$  states from Si in silicide, in particular, in the top layer. At  $\bar{M}'$  and  $\bar{K}'$ , erbium largely dominates.  $S_2$  has a similar character at  $\bar{\Gamma}'$ , with mainly Er  $5d^2$  and Si  $3p_z$ . Off  $\bar{\Gamma}'$ , along the  $\bar{\Gamma}'\bar{M}'$  direction, the band acquires progressively dominant Si  $3p_z$  states from the buckled Si top layer, reflecting mainly the Si dangling bonds.  $S_4$  presents a similar character along the  $\bar{\Gamma}'\bar{M}'$  line and at  $\bar{K}'$ . Actually, both bands reflect the Si dangling-bond states. The similar content of bands  $S_2$  and  $S_4$  is easily explained if one considers that they derive from the  $p(1 \times 1)$  2D bands folded back into the reduced  $\sqrt{3} \times \sqrt{3} R30^\circ$  zone, and that, because of the  $\sqrt{3} \times \sqrt{3}$  perturbation, a gap is opened at  $\bar{M}'$ .<sup>12</sup> Band  $S_3$  is only visible in the experiment near  $\bar{M}'$ . At this point, we find hybridization between Er  $5d_{xy}$  states from both Er layers and Si  $3p_z$  states from Si atoms of the terminal bilayer, as well as of the graphitelike Si plane between the 2-Er layers. This band is a resonance of bulklike Si- $\pi$  states and will be discussed in detail elsewhere.

#### IV. CONCLUSION

We have compared the experimental and theoretical surface band structure for 2 Er silicide layers grown on  $\text{Si}(111)$ . Various surface atomic configurations have been tested. Agreement is obtained for geometries consisting of a reconstructed  $\text{ErSi}_{1.7}$  silicide surface termination with  $\text{ErSi}_2$  stoichiometry. Our calculations show that the hypothesis of a surface termination with  $\text{ErSi}_{1.7}$

stoichiometry, i.e., with vacancies in the buckled Si top layer, as well as the hypothesis of a flat Si top layer with or without vacancies, are incompatible with experiment and can, therefore, be safely ruled out.

The surface structure without vacancies are also the ones expected from simple reasoning in terms of dangling bonds. Indeed, as pointed out in previous work<sup>9,20</sup> in a buckled top layer, the Si dangling bonds are formally doubly occupied, because one electron is transferred from Er to Si. This results in a particularly stable and inert surface. If one introduces one Si vacancy per  $\sqrt{3}$  unit cell, one replaces one topmost dangling bond per  $\sqrt{3}$  unit cell by three dangling bonds in the second Si layer. The latter lie lower in energy, because of their bonding interaction, so that the saturation of these low-lying dangling bonds already needs the 3 electron/ $\sqrt{3}$  cell available from Er donation. Hence the two remaining dangling bonds in the topmost layer must be singly occupied.

This would result in a very unstable surface quite similar to ideal Si(111)(1×1) surface. From the band-structure point of view, this means that there would be essentially one occupied band derived from the topmost Si dangling bonds (in the  $\sqrt{3}$  SBZ), as opposed to three in the absence of vacancies. Finally, we find again that the simple EHT method proves to be very useful in testing various atomic arrangements in spite of the rough approximations involved in this semiempirical technique. In this respect, it is noteworthy that the structural model  $M_1$  arrived at in the present study has indeed been confirmed very recently by scanning tunneling microscopy.<sup>21</sup>

#### ACKNOWLEDGMENT

The Laboratoire de Physique et de Spectroscopie Electronique is Unité de Recherche Associée au CNRS No. 1435.

- 
- <sup>1</sup>J. A. Knapp and S. T. Picraux, *Appl. Phys. Lett.* **48**, 466 (1986).
- <sup>2</sup>K. N. Tu, R. D. Thompson, and B. Y. Tsaur, *Appl. Phys. Lett.* **38**, 626 (1981).
- <sup>3</sup>F. Hellman and R. T. Tung, *Phys. Rev. B* **37**, 10 786 (1988).
- <sup>4</sup>F. Arnaud d'Avitaya, A. Perio, J. C. Oberlin, Y. Campidelli, and J. A. Chroboczek, *Appl. Phys. Lett.* **54**, 2198 (1989).
- <sup>5</sup>F. H. Kaatz, J. Van der Spiegel, and W. R. Graham, *J. Appl. Phys.* **69**, 514 (1991).
- <sup>6</sup>F. P. Netzer, *J. Phys. Condens. Matter* (to be published), and references therein.
- <sup>7</sup>P. Wetzel, C. Pirri, P. Paki, D. Bolmont, and G. Gewinner, *Phys. Rev. B* **47**, 3677 (1993).
- <sup>8</sup>M. H. Tuilier, P. Wetzel, C. Pirri, D. Bolmont, and G. Gewinner, *Phys. Rev. B* **50**, 2333 (1994).
- <sup>9</sup>L. Stauffer, A. Mharchi, C. Pirri, P. Wetzel, D. Bolmont, G. Gewinner, and C. Minot, *Phys. Rev. B* **47**, 10 555 (1993).
- <sup>10</sup>R. Baptist, S. Ferrer, G. Grenet, and H. C. Poon, *Phys. Rev. Lett.* **64**, 311 (1990).
- <sup>11</sup>J. Y. Veuillen, T. A. Nguyen Tan, and D. B. B. Lollman, *Surf. Sci.* **293**, 86 (1993).
- <sup>12</sup>P. Wetzel, S. Saintenoy, C. Pirri, D. Bolmont, and G. Gewinner, *Phys. Rev. B* **50**, 10 886 (1994).
- <sup>13</sup>P. Paki, U. Kafader, P. Wetzel, C. Pirri, J. C. Peruchetti, D. Bolmont, and G. Gewinner, *Phys. Rev. B* **45**, 8490 (1992).
- <sup>14</sup>S. Saintenoy, P. Wetzel, C. Pirri, D. Bolmont, and G. Gewinner, *Surf. Sci.* **331-333**, 546 (1995).
- <sup>15</sup>R. Hoffman, *J. Chem. Phys.* **39**, 1399 (1963).
- <sup>16</sup>M. H. Wangbo and R. Hoffmann, *J. Am. Chem. Soc.* **100**, 6093 (1978); C. Minot, M. A. Van Hove, and G. A. Somorjai, *Surf. Sci.* **127**, 441 (1983).
- <sup>17</sup>R. Hoffmann and P. Hofmann, *J. Am. Chem. Soc.* **98**, 598 (1976); J. H. Ammeter, H. B. Brügi, J. Thibeault, and R. Hoffmann, *ibid.* **100**, 3686 (1976).
- <sup>18</sup>M. H. Tuilier, C. Pirri, P. Wetzel, G. Gewinner, J. Y. Veuillen, and T. A. Nguyen Tan, *Surf. Sci.* **307-309**, 710 (1994).
- <sup>19</sup>M. Lohmeier, Ph.D. thesis, Amsterdam, Netherlands, 1995.
- <sup>20</sup>P. Wetzel, C. Pirri, P. Paki, J. C. Peruchetti, D. Bolmont, and G. Gewinner, *Solid State Commun.* **82**, 235 (1992).
- <sup>21</sup>T. P. Roge, F. Palmino, C. Savall, J. C. Labrune, P. Wetzel, C. Pirri, and G. Gewinner, *Phys. Rev. B* **51**, 10 998 (1995).

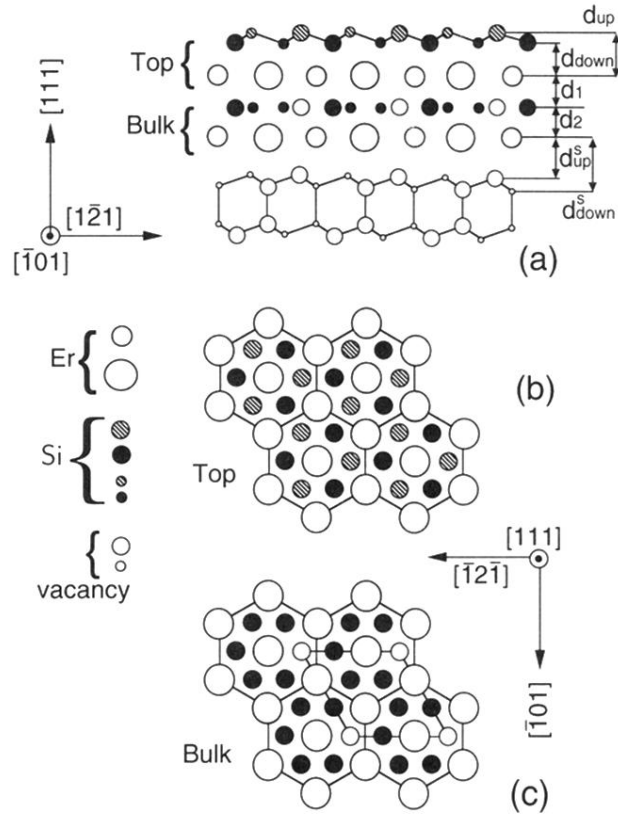


FIG. 2. Typical structure of the slab used in the band calculations for a 2 ML of Er disilicide. (a) Side view, the smaller circles indicate atoms lying out of the plane of the paper. (b) Sketch of reconstructed top silicide layer. (c) The underlying bulklike silicide layer. The Si substrate is modeled by an  $n$ -atomic-double-layer slab with backface dangling bonds saturated by one-orbital atoms.